

Study of superlattice-based phonon filters and cavities

Yu Cao* and Debdeep Jena†

Department of Electrical Engineering, University of Notre Dame, IN, 46556, USA

(Dated: December 11, 2006)

The theory of transfer matrix is used for the calculation of acoustic-phonon transmission through a periodic AlN/GaN-based superlattice with a finite number of periods. The results are applied to the design of broadband phonon filters and single-mode phonon cavities. The resonance phenomena of phonons is found in the triple-superlattice and superlattice-single layer-superlattice cavity structures.

INTRODUCTION

Resonant cavities have been studied since 1877, when Lord Rayleigh published his Theory of Sound. They have achieved great achievements in optics fields. Fabry and Perot cavity is a notable example. With distributed Bragg reflectors (DBR) combined, Fabry and Perot optical cavity is widely used as a light filter, such as single-wavelength photo-detector, or a container for photons with a certain wavelength, such as used in LASERS. Fig 1 shows a layer structure for a single-wavelength photodetector[1]. As designed, only the light with wavelength of 1542nm can pass through the cavity and DBRs, reaching the p-i-n region underneath. The reflection spectrum is shown in Fig 2.

The DBR structure is composed with periodic units to enhance the selectivity of wavelength. In each unit, there are two layers A and B with different refractive indices. The thickness of each unit is equal to half of the wavelength λ_p to be passed through. So the thickness of layer A and B may be $\lambda_p/4$ separately. The thickness of the

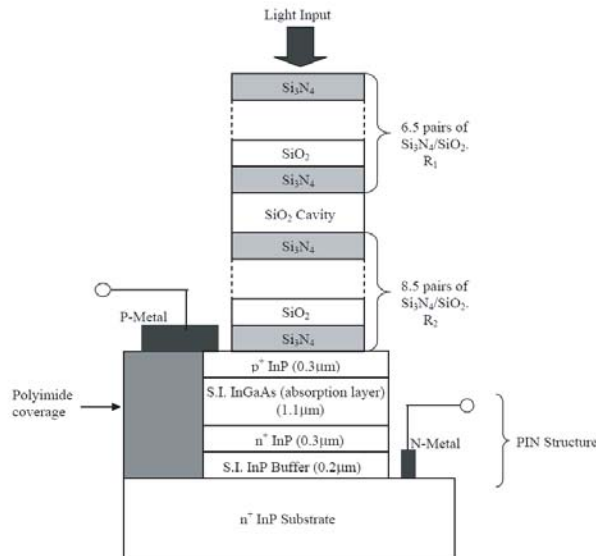


FIG. 1: Photon cavity for single-wavelength photo-detector application

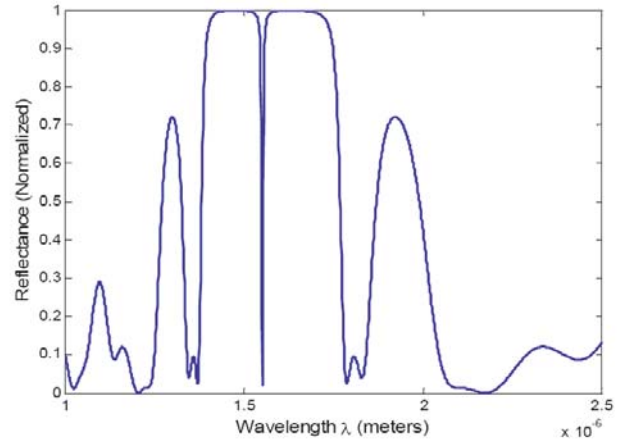


FIG. 2: Simulated reflection spectra for the photon cavity depicted in Fig 1

cavity is also the half of the λ_p . The more periods used in DBR, the better the light is filtered. But considering the dissipation of light in the DBRs, too many periods is not desired. So selecting the material for layers with large difference in the refractive indices is also helpful to enhance the filtering effect.

Phonons are similar with photons in some sense. Both of them are waves with a certain wavelength and have reflection or transmission spectra between different materials. Since phonon is actually the vibration of lattice atoms, instead of being related with refractive index in optical materials, the transmission of phonons depends more on the atom mass of the layer where they are propagating.

Device researchers are interested in acoustic phonons because they are related with the energy dissipation and lattice heating during the device operation. And by designing proper phonon cavities, it is possible to create directional energy flow of lattice excitations in active electronic devices.

Trigo et al.[2, 3] have performed the first studies of the scattering of standing-wave photons from standing-wave phonons by placing an acoustic phonon cavity inside an optical cavity, which is used to enhance the interaction between photons and phonons. The structure is shown

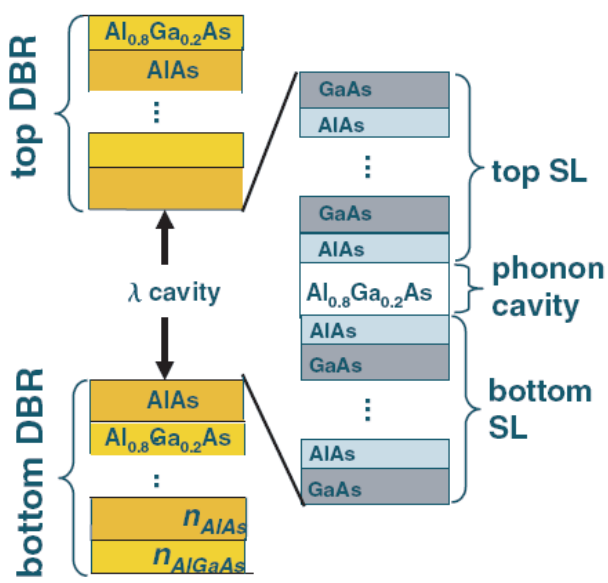


FIG. 3: Scheme of the phonon cavity embedded within an optical cavity

in Fig 3. Their research shows the possibility for the generation of coherent phonons. The thickness of the phonon cavity is $\lambda_{ac}/2$, where λ_{ac} is the wavelength of the acoustical phonon at the center of the phonon minigap.

Raman spectrum can be used to analyze the phonon mode staying in the cavity. But applying Transfer Matrix Method, the phonon reflectivity and Raman spectrum for the above phonon cavity can both be calculated, which is shown in Fig 4.

Studies on acoustic phonon in nitrides are of special interests because nitride devices are normally used for high-power applications. Device heating is an important issue. In this paper, we study the transmission behavior of acoustic phonons in AlN/GaN-based superlattices. Phonon filter and cavity are designed according to the simulation results using transfer matrix method.

THEORY

Two methods for the calculation of acoustic-wave transmission in semiconductor superlattices have been widely used: Transfer matrix model and Kronig-Penny model.

Transfer matrix method allows one to reproduce the infinite periodic system features (dispersion relations, stop bands, etc.), by means of N repeated bilayers, if N is sufficiently large. This means instead of solving a secular equation in a number of eigenvalues which corresponds to the number of interfaces, it is possible to obtain the same results by solving an inhomogeneous 6×6 system in the unknowns transmission rate T and reflection rate

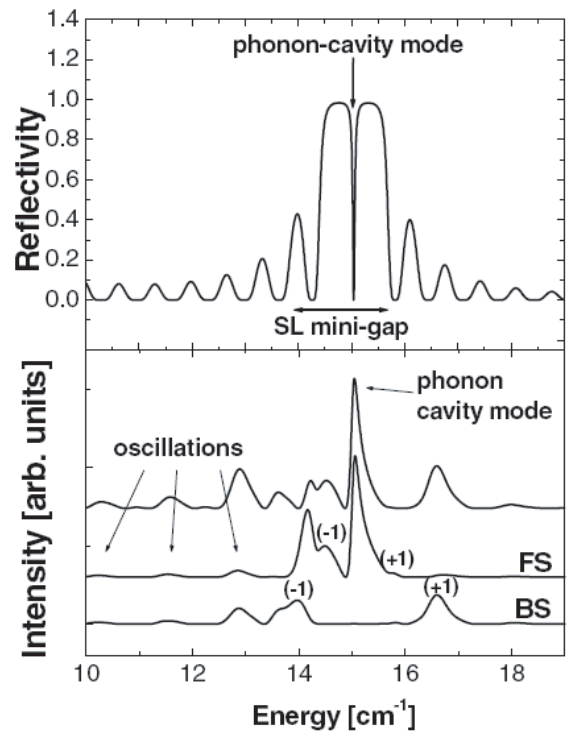


FIG. 4: Calculated phonon reflectivity (top) and Raman spectrum (bottom) in the spectral region around the first zone-center minigap for the phonon cavity embedded within a photon cavity depicted in Fig 3

R . This method is numerically simple, and it is then possible to be extended to more complicated systems, such as multilayered structures, without increasing the dimension of the transfer matrix.

The elastic analogue of Kronig-Penny model is widely used for the study of the dispersion curves in superlattices, i.e., a monodimensional method which can be applied only along directions of propagation for which the phonon velocity is well defined.

In this paper, we are going to use the transfer matrix method developed by S. Mizuno and S. Tamura[4]. For the completeness of this report, the method is introduced as below.

A periodic superlattice with a finite number of periods is studied. The schematic picture of this structure is shown in Fig 5. We assume that the superlattice consists of a periodic sequence of alternate stacking of A_1 and A_2 layers. The thicknesses of the A_1 and A_2 layers are denoted by d_{A_1} and d_{A_2} , respectively, and D_A ($=d_{A_1} + d_{A_2}$) is the thickness of the unit period of this system.

We consider the case where the phonon wave vector is parallel to the growth direction (z direction). For this propagation configuration all three phonon modes (shear horizontal (SH), shear vertical (SV) and longitudinal (L)) are decoupled from each other if the interfaces are a

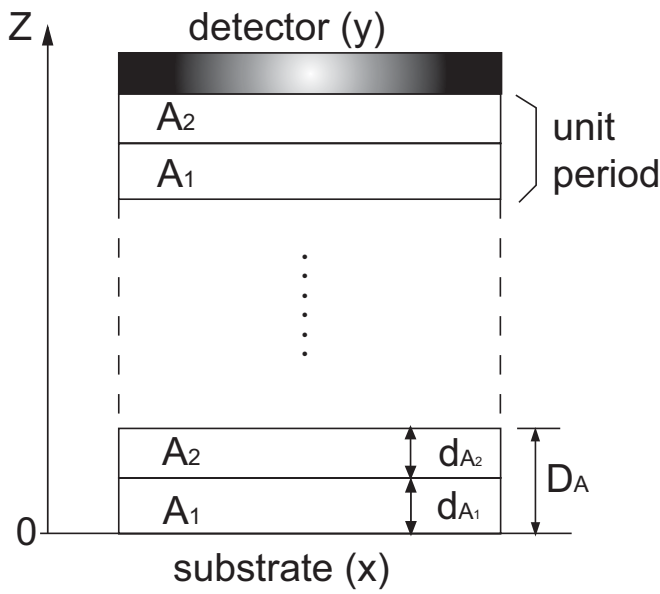


FIG. 5: Schematic picture of the periodic superlattice with the N periods

mirror-symmetry plane. We take such a simple situation but treat only one mode of phonons. We adopt the continuum model for the lattice vibration, which is valid for sub-THz acoustic phonons in most of the semiconductor superlattices. The solution to the one-dimensional wave equation for this elastic continuum is expressed in terms of a linear combination of the transmitted and reflected waves:

$$U_i(z) = c_i^t e^{ik_i z} + c_i^r e^{-ik_i z}, \quad (1)$$

where i is an index specifying constituent layers, c_i^t and c_i^r are the amplitudes of the transmitted and reflected waves, respectively, and k_i is the wave number. The stress associated with the lattice displacement U_i is

$$S_i(z) = i\omega Z_i (c_i^t e^{ik_i z} - c_i^r e^{-ik_i z}), \quad (2)$$

where $Z_i (= \rho_i v_i)$ is the acoustic impedance with the mass density ρ_i and the sound velocity v_i , and $\omega = k_i v_i$ is the angular frequency.

The boundary condition for this system is the continuity of the lattice displacement $U_i(z)$ and stress $S_i(z)$ across the interfaces of adjacent layers. For the convenience of writing these boundary conditions, we can introduce a two-component vector

$$W_i(z) = \begin{bmatrix} U_i(z) \\ S_i(z) \end{bmatrix}. \quad (3)$$

Let us consider the first layer A_1 , which is sandwiched by the substrate denoted by x and the second layer A_2 (see Fig 5). The boundary conditions require

$$W_{A_1}(0) = W_x(0) \quad (4)$$

and

$$W_{A_1}(d_{A_1}) = W_{A_2}(d_{A_1}) \quad (5)$$

By the Eqn 1 and Eqn 2, $W_i(z)$ can be written as

$$W_i(z) = \underline{h}_i(z) C_i, \quad (6)$$

where

$$\underline{h}_i = \begin{bmatrix} e^{ik_i z} & e^{-ik_i z} \\ i\omega Z_i e^{ik_i z} & -i\omega Z_i e^{-ik_i z} \end{bmatrix} \quad (7)$$

and

$$C_i = \begin{bmatrix} c_i^t \\ c_i^r \end{bmatrix}. \quad (8)$$

Using Eqn 6, we can combine Eqn 4 and Eqn 5 and get

$$W_{A_2} = \underline{t}_{A_1}(d_{A_1}) W_x(0), \quad (9)$$

where

$$\underline{t}_{A_1} = \underline{h}_{A_1}(d_{A_1}) [\underline{h}_{A_1}(0)]^{-1}. \quad (10)$$

This means that W changes to $\underline{t}_{A_1} W$ after the propagation of a wave through the first layer A_1 . Let $\alpha_1 = k_{A_1} d_{A_1}$. $\underline{t}_{A_1}(d_{A_1})$ can be written as

$$\underline{t}_{A_1}(d_{A_1}) = \begin{bmatrix} \cos\alpha_1 & \frac{1}{\omega Z_{A_1}} \sin\alpha_1 \\ -\omega Z_{A_1} \sin\alpha_1 & \cos\alpha_1 \end{bmatrix}. \quad (11)$$

Similarly, we can define the matrix \underline{t}_{A_2} for the A_2 layer. Using \underline{t}_{A_1} and \underline{t}_{A_2} , we can relate W 's right before and after one unit period consisting of A_1 and A_2 layers,

$$\underline{T}_{A_1} = \underline{t}_{A_1} \underline{t}_{A_2} \equiv \begin{bmatrix} \lambda_A & \frac{1}{\omega Z_{A_1}} \sigma_A \\ \omega Z_{A_1} \zeta_A & \mu_A \end{bmatrix}, \quad (12)$$

where

$$\lambda_A = \cos\alpha_1 \cos\alpha_2 - \frac{Z_{A_1}}{Z_{A_2}} \sin\alpha_1 \sin\alpha_2, \quad (13)$$

$$\sigma_A = \sin\alpha_1 \cos\alpha_2 + \frac{Z_{A_1}}{Z_{A_2}} \cos\alpha_1 \sin\alpha_2, \quad (14)$$

$$\zeta_A = -\sin\alpha_1 \cos\alpha_2 - \frac{Z_{A_2}}{Z_{A_1}} \cos\alpha_1 \sin\alpha_2, \quad (15)$$

$$\mu_A = \cos\alpha_1 \cos\alpha_2 - \frac{Z_{A_2}}{Z_{A_1}} \sin\alpha_1 \sin\alpha_2, \quad (16)$$

with $\alpha_2 = k_{A_2} d_{A_2}$.

For the superlattice with N periods, we need to calculate $(\underline{T}_A)^N \equiv \underline{T}_A(N)$. To obtain the analytical expression of $\underline{T}_A(N)$, we need to transform \underline{T}_A into the diagonal matrix $\tilde{\underline{T}}_A$:

$$\tilde{\underline{T}}_A = \underline{S}^{-1} \underline{T}_A \underline{S} = \begin{bmatrix} \epsilon_1 & 0 \\ 0 & \epsilon_2 \end{bmatrix}, \quad (17)$$

where ϵ_1 and ϵ_2 are the solutions of the equation

$$\epsilon^2 - (\mu_A + \lambda_A)\epsilon + 1 = 0. \quad (18)$$

Solving the above equation, we can explicitly express the transfer matrix $\underline{T}_A(N)$ for the following three cases.

(a) $|(\mu_A + \lambda_A)/2| \leq 1$. We define

$$\cos \theta_A \equiv \frac{\mu_A + \lambda_A}{2}. \quad (19)$$

Hence, $\epsilon_{1,2}$ can be written as

$$\epsilon_{1,2} = \cos \theta_A \pm i \sin \theta_A = e^{\pm i \theta_A}, \quad (20)$$

and the corresponding matrix \underline{S} is given by

$$\underline{S} = \begin{bmatrix} -\sigma_A & -\sigma_A \\ \lambda_A - e^{i\theta_A} & \lambda_A - e^{-i\theta_A} \end{bmatrix}, \quad (21)$$

With Eqn 17 and Eqn 21, $\underline{T}_A(N)$ is calculated as

$$\begin{aligned} \underline{T}_A(N) &\equiv (\underline{T}_A)^N = \underline{S}(\underline{\tilde{T}}_A)^N \underline{S}^{-1} \\ &= \begin{bmatrix} \frac{\lambda_A - \mu_A}{2} S_A(N) + C_A(N) & \frac{1}{\omega Z_{A1}} \sigma_A S_A(N) \\ \omega Z_{A1} \zeta_A S_A(N) & -\frac{\lambda_A - \mu_A}{2} S_A(N) + C_A(N) \end{bmatrix}, \end{aligned} \quad (22)$$

where

$$S_A(N) \equiv \frac{\sin(N\theta_A)}{\sin \theta_A}, \quad (23)$$

$$C_A(N) \equiv \cos(N\theta_A). \quad (24)$$

(b) $(\mu_A + \lambda_A)/2 > 1$. We define θ_A by

$$\cosh \theta_A \equiv \frac{\mu_A + \lambda_A}{2}. \quad (25)$$

Then, $\epsilon_{1,2}$ can be written as

$$\epsilon_{1,2} = \cosh \theta_A \pm \sinh \theta_A = e^{\pm \theta_A}, \quad (26)$$

and $\underline{T}_A(N)$ has the same form as Eqn 22, but with

$$S_A(N) \equiv \frac{\sinh(N\theta_A)}{\sinh \theta_A}, \quad (27)$$

$$C_A(N) \equiv \cosh(N\theta_A). \quad (28)$$

(c) $(\mu_A + \lambda_A)/2 < -1$. In this case, we define θ_A by

$$\cosh \theta_A \equiv \frac{\mu_A + \lambda_A}{2}. \quad (29)$$

Then, $\epsilon_{1,2}$ can be written as

$$\epsilon_{1,2} = -\cosh \theta_A \mp \sinh \theta_A = -e^{\pm \theta_A}, \quad (30)$$

and $\underline{T}_A(N)$ has the same form as Eqn 22, but with

$$S_A(N) \equiv (-1)^{N+1} \frac{\sinh(N\theta_A)}{\sinh \theta_A}, \quad (31)$$

$$C_A(N) \equiv (-1)^N \cosh(N\theta_A). \quad (32)$$

Next we can calculate the phonon transmission rate by applying the above analytical expressions for the transfer matrix. It is assumed that the high-frequency phonons are excited at the back of the substrate x. Thus both the incident and reflected phonons exist in the substrate but there are only transmitted phonons in the detector layer. Thus for an incident phonon with unit displacement amplitude, we have

$$W_x(z) = \underline{h}_x(z) \begin{bmatrix} 1 \\ c_x^r \end{bmatrix} \quad (33)$$

in the substrate and

$$W_y(z) = \underline{h}_y(z) \begin{bmatrix} c_y^t \\ 0 \end{bmatrix} \quad (34)$$

in the detector layer. The amplitudes of reflection c_x^r and transmission c_y^t are determined by the continuity condition for W at each layer interface. Applying the transfer matrix $T_A(N)$, this condition yields

$$W_y(ND_A) = \underline{T}_A(N)W_x(0). \quad (35)$$

Define

$$a = \frac{\lambda_A - \mu_A}{2} S_A(N) + C_A(N), \quad (36)$$

$$b = \sigma_A S_A(N), \quad (37)$$

$$c = \zeta_A S_A(N), \quad (38)$$

$$d = -\frac{\lambda_A - \mu_A}{2} S_A(N) + C_A(N). \quad (39)$$

Then $\underline{T}_A(N)$ can be written as

$$\underline{T}_A(N) = \begin{bmatrix} a & \frac{1}{\omega Z_{A_1}} b \\ \omega Z_{A_1} c & d \end{bmatrix}. \quad (40)$$

Accordingly, from Eqn 33, 34 and 35, we have

$$c_y^t = \frac{2i}{\left(\frac{Z_y}{Z_{A_1}} b - \frac{Z_{A_1}}{Z_x} c\right) + i\left(d + \frac{Z_y}{Z_x} a\right)} e^{-ik_y N D_A}, \quad (41)$$

$$c_x^r = \frac{\left(\frac{Z_y}{Z_{A_1}} b + \frac{Z_{A_1}}{Z_x} c\right) + i\left(d - \frac{Z_y}{Z_x} a\right)}{\left(\frac{Z_y}{Z_{A_1}} b - \frac{Z_{A_1}}{Z_x} c\right) + i\left(d + \frac{Z_y}{Z_x} a\right)}. \quad (42)$$

The energy transmission rate T and reflection rate R are defined by

$$T \equiv \frac{Z_y}{Z_x} |c_y^t|^2, \quad (43)$$

$$R \equiv |c_x^r|^2. \quad (44)$$

From Eqn 41 and 42, we get

$$T = \frac{4 \frac{Z_y}{Z_x}}{\left(\frac{Z_y}{Z_{A_1}} b - \frac{Z_{A_1}}{Z_x} c\right)^2 + \left(d + \frac{Z_y}{Z_x} a\right)^2}, \quad (45)$$

$$R = \frac{\left(\frac{Z_y}{Z_{A_1}} b + \frac{Z_{A_1}}{Z_x} c\right)^2 + \left(d - \frac{Z_y}{Z_x} a\right)^2}{\left(\frac{Z_y}{Z_{A_1}} b - \frac{Z_{A_1}}{Z_x} c\right)^2 + \left(d + \frac{Z_y}{Z_x} a\right)^2}. \quad (46)$$

If multiple superlattices are stacked, the total transfer matrix can be expressed as

$$\underline{T}_{total} \equiv \prod_{i=1}^n \underline{T}_i, \quad (47)$$

where i is the index for each superlattice. Applying equations similar with Eqn 33, 34 and 35, the amplitude of total reflection c_x^r and total transmission c_y^t can be extracted. Inductively we have the total reflection rate R_{total} and transmission rate T_{total} .

NUMERICAL SIMULATION

Single Superlattice

Single superlattice can behave as a phonon filter. As a numerical example, we choose a (100) AlN/GaN superlattice and consider two periodic superlattices A-type and B-type, whose unit periods consists of (6 ML AlN)/(6 ML GaN) and (9 ML AlN)/(9 ML GaN), respectively. The number of periods in the A(B) superlattice is $N = 35$ ($M = 35$). In Fig 6, we show the frequency dependence of the longitudinal phonon transmission rates in these periodic superlattices calculated from Eqn 40 and 45. The figure shows two dips of the transmission rate, one is around 1THz, the other is around 1.5THz. This means the phonons with the frequency in these ranges are all reflected before reaching the detector layer.

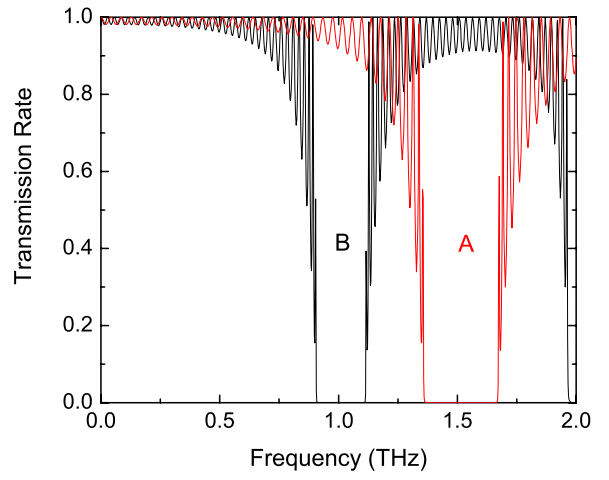


FIG. 6: Frequency dependence of the L-phonon transmission rate in (100) AlN/GaN superlattices: A-type superlattice (6 ML AlN/6 ML GaN) and B-type superlattice (9 ML AlN/9 ML GaN). Both the superlattices have 35 periods. The mass density and longitudinal sound velocity are 3.23 g/cm³ and 10.97 km/s for AlN, and 6.15 g/cm³ and 8.04 km/s for GaN.

Multiple Superlattice

If multiple superlattices are stacked, the total transmission rate can be extracted from the total transfer matrix, which is the products of that for each superlattice. It can be foreseeable that we actually have multiple phonon filters working together. The phonons with frequencies in either stop band of these superlattices can not get transmitted. This is proved by numerical calculation which is shown in Fig 7, where two superlattices are stacked

If more than two superlattices are stacked and well-designed such that some part of their stop bands overlaps with others, we could have a phonon filter with a "broad" stop band, which is useful for phonon cavity design if we want to hold as many longitudinal phonons as possible. Fig 8 shows the case where four AlN/GaN superlattices (AlN₆/GaN₆, AlN₇/GaN₇ and AlN₈/GaN₈) are stacked. Each of these superlattices have 15 periods.

Superlattice-based Cavities

The study of phonon cavity is attractive because it can provide single mode transmission. For example, if we have a stack of superlattice with the structure of ABA, where A-type superlattice is with 6 ML AlN/6 ML GaN and B-type superlattice is with 9 ML AlN/9 ML GaN. The periods number for A and B are 10 and 15 respectively. The total transmission rate is plotted in Fig 9. The most noticeable feature is the appearance of three

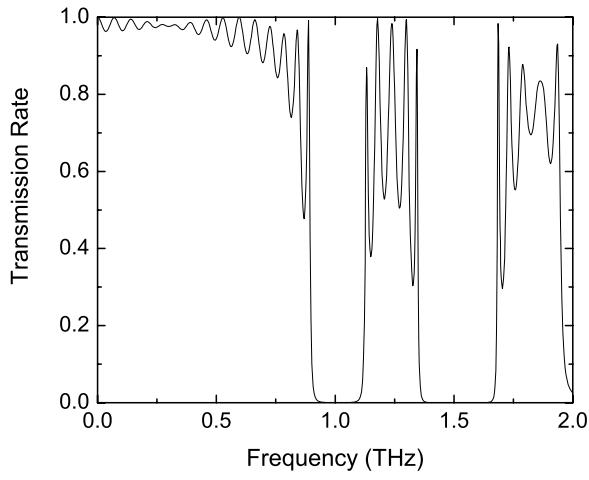


FIG. 7: Frequency dependence of the L-phonon transmission rate in the *AB* superlattice structure ($N=20$, $M=15$).

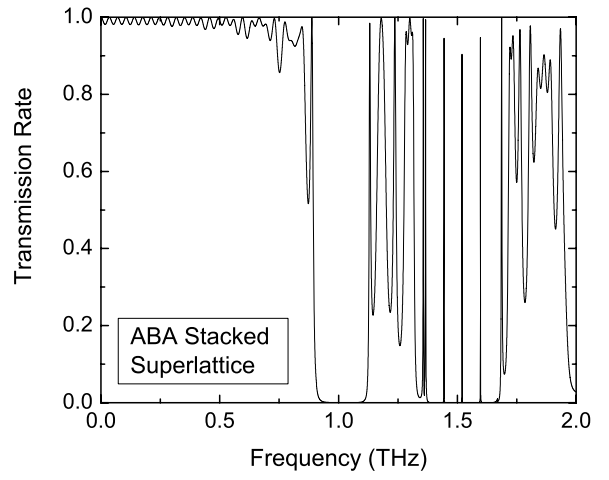


FIG. 9: Frequency dependence of the L-phonon transmission rate in the *ABA* superlattice structure ($N=10$, $M=15$).

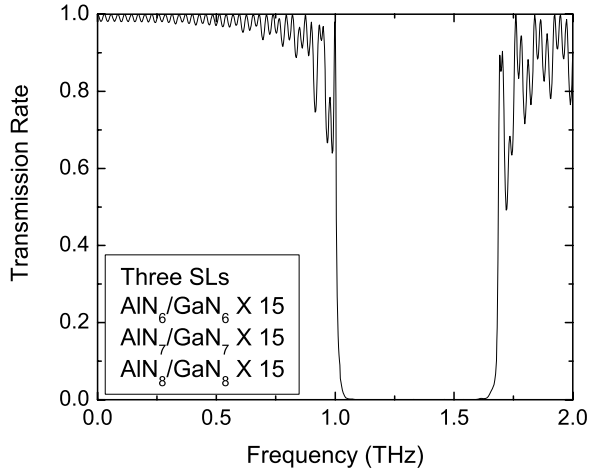


FIG. 8: Frequency dependence of the L-phonon transmission rate in the three-superlattice structure with 15 periods for each of them.

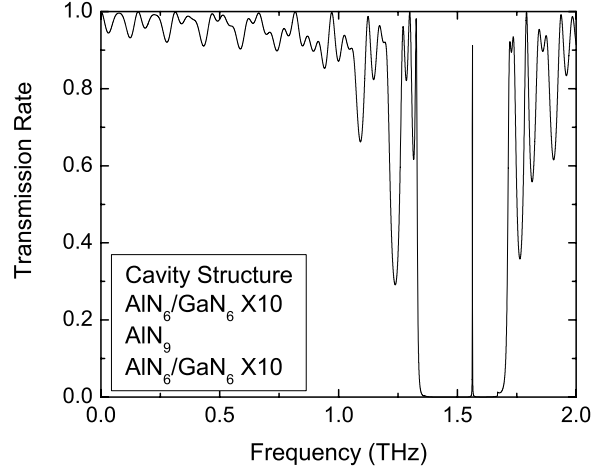


FIG. 10: Frequency dependence of the L-phonon transmission rate in the *A – Single – layer AlN – A* superlattice structure. A-type superlattice has 10 periods. The single layer AlN has 9 monolayers.

sharp enhancements in transmission in the stop band of A-type superlattice. These enhancements in transmission correspond to the resonant transmission.

If we use a single layer with the thickness of $\lambda_{ac}/2$ instead of the superlattice B in the above example, where λ_{ac} is the wavelength of the acoustic phonon at the center of the phonon minigap, we can have one phonon-cavity mode in the stop band of superlattice A, which is shown in Fig ?? . An enlarged view for the phonon-cavity mode is also shown in Fig 11.

CONCLUSION

The transmission rate is calculated for AlN/GaN based single superlattice, a stack of different superlattices. A broadband phonon filter is proposed by stacking three different superlattice. The transmission for the phonon cavity is also calculated, which shows the existence of phonon-cavity modes in the stop band of the superlattice. These modes are due to the resonant transmission in the

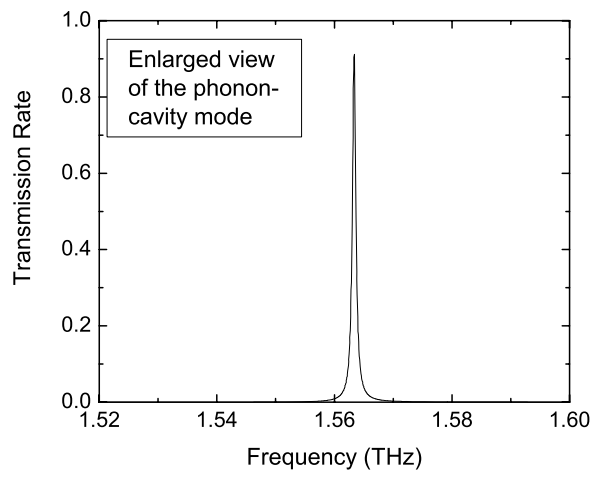


FIG. 11: Enlarged view of the phonon-cavity mode in the A - *Single-layer AlN* - A superlattice structure shown in Fig 10.

proposed cavity structures.

* Electronic mail: ycao1@nd.edu

† Electronic mail: djena@nd.edu

- [1] S. Vicknesh, Y. Cao and A. Ramam, Proc. SPIE, Infrared and Photoelectronic Imagers and Detector Devices II **6294**, 62940K (2006).
- [2] M. Trigo, A. Bruchhausen, A. Fainstein, B. Jusserand, and V. Thierry-Mieg, Phys. Rev. Lett. **89**, 227402 (2002).
- [3] A. Fainstein, B. Jusserand, and V. Thierry-Mieg, Phys. Rev. Lett. **75**, 3764 (1995).
- [4] S. Mizuno and S. Tamura, Phys. Rev. B **45**, 45734 (1992).